Journal of Power Sources 181 (2008) 155–160

Contents lists available at ScienceDirect

Journal of Power Sources

journal homepage: www.elsevier.com/locate/jpowsour

Short communication

# Battery performances and thermal stability of polyacrylonitrile nano-fiber-based nonwoven separators for Li-ion battery

Tae-Hyung Cho[a,*], Masanao Tanaka[b], Hiroshi Onishi[b], Yuka Kondo[b], Tatsuo Nakamura[b], Hiroaki Yamazaki[b], Shigeo Tanase[a], Tetsuo Sakai[a,**]

[a] National Institute of Advanced Industrial Science and Technology, Kansai, 1-8-31 Midorigaoka, Ikeda, Osaka 563-8577, Japan
[b] Japan Vilene Co., Ltd., 7 Kita-Tone, Koga, Ibaraki 306-0213, Japan

ARTICLE INFO

*Article history:*
Received 8 January 2008
Received in revised form 3 March 2008
Accepted 3 March 2008
Available online 14 March 2008

*Keywords:*
Li-ion battery
Polyacrylonitrile nano-fiber
Nonwoven separator
Electrospinning

ABSTRACT

The microporous polyacrylonitrile (PAN) nonwoven separators have been developed by using electrospun nano-fibers with homogeneous diameter of 380 and 250 nm. The physical, electrochemical and thermal properties of the PAN nonwovens were characterized. The PAN nonwovens possessed homogeneous pore size distribution with similar pore size to the conventional microporous membrane separator. Moreover, the PAN nonwovens showed higher porosities, lower gurley values and better wettabilities than the conventional polyolefin microporous separator. Cells with the PAN nonwovens showed better cycle lives and higher rate capabilities than that of a cell with conventional one. Any internal short circuit was not observed for the cells with the PAN nonwovens during charge–discharge test. Hot oven tests for the charged cells up to 4.2 V have revealed that the PAN nonwoven was thermally stable at 120 °C, but showed shrinkage of about 26% isotropically after the test at 150 °C for 1 h. The Celgard membrane showed uniaxial shrinkage of about 30% along the machine direction at 150 °C for 1 h.



## 1. Introduction

A separator is totally necessary in order to separate positive and negative electrode and maintaining liquid electrolyte between both of the electrodes. However, the existence of the separator increases cell resistance by a factor of 6–7 [1] and reduces volumetric energy density of the battery. Polyolefin microporous membranes have been used as major separator for the lithium ion battery. But, the rate capabilities of the separators are not enough for high power application, such as electric vehicles, hybrid electric vehicles and robots. The microporous membrane separators have some disadvantages to be improved, e.g. low wettability [2,3] and low porosity of about 40% [4]. On the contrary, nonwoven separators have higher porosity (60–90%) and higher air permeability than the polyolefin one, which would increase the rate capability of the lithium ion battery. However, the nonwoven separators have some disadvantages, such as large pore size and thicker nature. Therefore, it is very worth developing a new nonwoven separator with small pore size, small volume, high porosity and high air permeability for high power lithium ion battery.

In our previous work [5], we have developed polyacrylonitrile (PAN) nano-fiber-based nonwoven separators with close thickness and similar pore size to the conventional microporous membrane one and similar porosity and air permeability to the conventional nonwoven one. The PAN nonwoven separators have exhibited outstanding battery performances, such as long cycle life and high rate capability. Recently, we have manufactured several series of the PAN nonwoven with different pore size by using different PAN nano-fibers (250 and 380 nm in diameters). In this paper, we report the physical, thermal and electrochemical properties of the PAN nonwovens as separator for lithium ion battery in detail.

## 2. Experimental

The PAN nonwovens discussed in this study were manufactured by using electrospun fine PAN fibers with 380 and 250 nm in diameters. Details for preparation of the PAN nonwoven were described in the previous report [5].

The morphologies of the electrospun PAN nano-fibers at fresh and after tests, e.g. charge–discharge test and hot oven test, were observed by scanning electron microscope (SEM). For the observation after tests, the separators were washed by using dimethyl carbonate (DMC). The mean pore sizes and pore size distributions of the PAN nonwovens were measured by using bubble point method [5]. The wettabilities of the PAN nonwoven and a conventional poly-

* Corresponding author. Tel.: +81 72 751 9611; fax: +81 72 751 9623.
** Corresponding author. Fax: +81 72 751 9623.
*E-mail addresses:* taehyung-cho@aist.go.jp (T.-H. Cho), sakai-tetsuo@aist.go.jp (T. Sakai).

0378-7753/$ – see front matter © 2008 Elsevier B.V. All rights reserved.
doi:10.1016/j.jpowsour.2008.03.010

olefin microporous membrane were estimated by monitoring the variation of contact angle between liquid electrolyte and the membranes at every 0.01 s by use of a high shutter speed camera.

Electrochemical characterizations were carried out using the CR-2032-type coin cell, which was composed of $LiCoO_2$ electrode as a cathode, graphite electrode (Hohsen Co. Ltd.) as an anode and 1 M $LiPF_6$-EC/DEC (1:1 in volume) as an electrolyte. Details for fabrication of the cathode and the coin cells were described in the previous report [5]. The electrochemical cycling tests were carried out in the voltage range of 3.0–4.2 V at 30 °C. In order to form a stable solid electrolyte interface (SEI) on the surface of the graphite anode, the first cycles for all of the test cells were charged under constant current–constant voltage (CC–CV) mode at the 0.2*C* rate, and then discharged under constant current mode at the 0.2*C* rate. In the following cycles, charge–discharge tests were carried out under constant current mode at the 0.5*C* rate. In order to investigate the discharge rate capability for the cells with various separators, the cells were charged up to 4.2 V at the 0.2*C* rate, and then discharged to 3.0 V at the *C* rates of 0.2, 0.5, 1, 2, 4 and 8*C*.

The ionic conductivities of the electrolyte with and without separators were measured by an a.c. impedance spectroscopy using HS cell (Hohsen, Japan). The cells were formed by sandwiching the electrolyte soaked separator between two stainless steel electrodes. The a.c. impedance measurements were carried out using Solatron SI 1280B frequency response analyzer (FRA). The impedances of the coin type cells were estimated at the fresh state and at the end of charge–discharge tests using the FRA over the frequency range of 20–0.1 Hz with 10 mV of the a.c. amplitude.

## 3. Results and discussion

### 3.1. Physical properties

In order to manufacture microporous nonwoven with small pore size and complex pore structure enough to prevent the internal short circuit during charge–discharge test, it is very important to use fine fibers with homogeneous diameter. The diameter and morphology of the electrospun nano-fiber are greatly influenced by electrospinning parameters, such as the polymer concentration, applied voltage, feeding speed of the polymer solution and capillary-screen distance [6]. We have prepared successfully fine PAN fibers with homogeneous diameters of around 250 and 380 nm by controlling these parameters. Fig. 1 shows SEM photographs of the nano-fibers. The fibers exhibited homogeneous diameters and any observable beads did not exist on the fibers.

Table 1 shows brief physical properties of the PAN nonwovens, compared with that of the conventional polypropylene membrane (Celgard® 2400). Hereinafter we refer the four PAN wonwovens as PAN No. 1–4. The PAN No. 1 and 2, which were made of 380 nm fibers, showed mean pore size of 0.28 and 0.38 μm, respectively. The mean pore sizes of the PAN nonwovens were reduced to 0.18 (PAN No. 3) and 0.17 μm (PAN No. 4) by using finer PAN fibers (250 nm) without remarkable decrease in the porosities. The measured thicknesses of the PAN nonwovens were in the range of 25–35 μm, of which values are similar to that of the Celgard membrane. In spite of similar thickness, the PAN nonwovens showed roughly two times higher porosities than that of the Celgard one. Besides, The PAN nonwovens showed enormously low gurley values compared with the Celgard one.

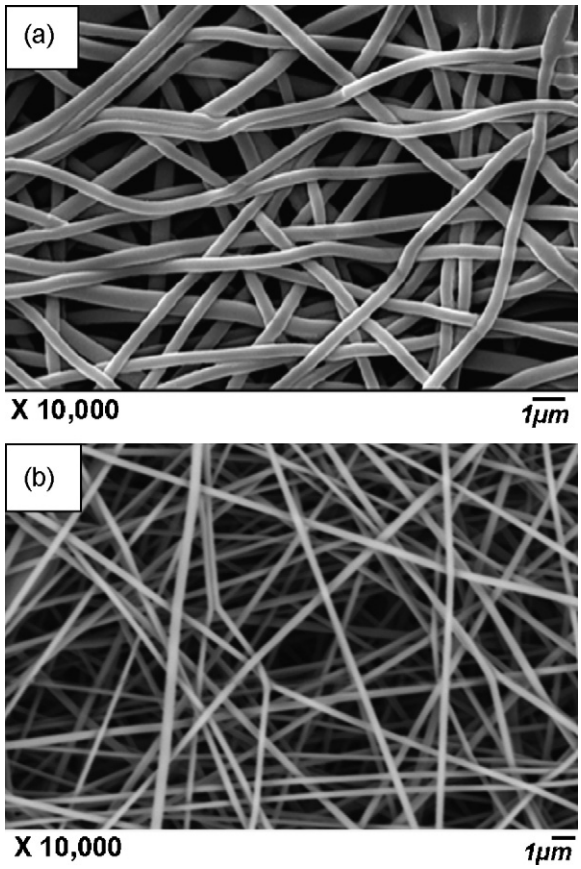


**Fig. 1.** SEM photographs of the electrospun PAN nano-fiber with diameter of (a) 380 nm and (b) 250 nm.

The wettability of the separator in non-aqueous electrolyte is important parameter because the separator with good wettability can retain the electrolyte effectively and facilitates an electrolyte to diffuse smoothly into the cell assembly [7]. The variations of the contact angles of the PAN nonwoven and the polyolefin membrane *versus* time are presented in Fig. 2. The contact angle of the PAN nonwoven decreased more rapidly than that of the polyolefin one. It means that the PAN nonwoven has better wettability than the polyolefin one. The better wettability of the PAN nonwoven could be ascribed to hydrophilicity of the PAN polymer.

### 3.2. Electrochemical properties

The existence of a separator between positive and negative electrodes causes the decrease in mobility of conductive ions during the

**Table 1**
Brief physical properties of separators

| Property | Celgard® 2400 | PAN No. 1 | PAN No. 2 | PAN No. 3 | PAN No. 4 |
|---|---|---|---|---|---|
| Composition | PP | PAN | PAN | PAN | PAN |
| Thickness (μm) | 25 | 33 | 35 | 25 | 30 |
| Pore size (μm) | 0.1 × 0.04 | 0.28 | 0.38 | 0.18 | 0.17 |
| Porosity[a] (%) | 37 | 64 | 76 | 64 | 56 |
| Gurley (sec./100 cc) | 730 | 7 | 3 | 9.5 | 11 |
| Fiber diameter (nm) | – | 380 | 380 | 250 | 250 |

[a] Calculated value for the PAN nonwoven membranes.

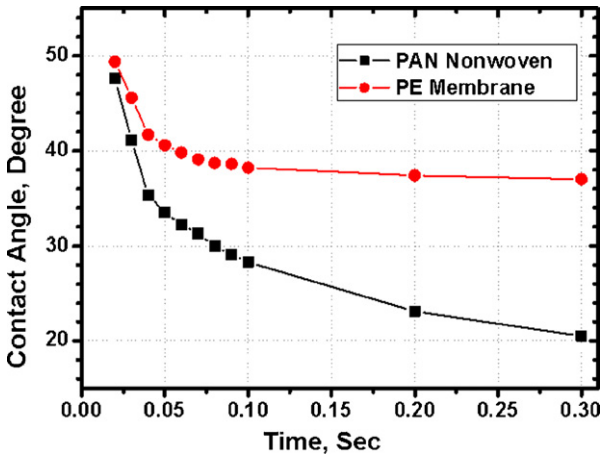


**Fig. 2.** Variation of contact angles between separators and electrolyte depending on time.

**Table 2**
The values of porosity, conductivities ($\sigma_{eff}$) and MacMullin number ($N_M$) obtained from conductivity measurement of separators

| Separator | Porosity (%) | $\sigma_{eff}$ (mS cm$^{-1}$) | $N_M$ |
|---|---|---|---|
| Celgard® 2400 | 37 | 0.8 | 12.0 |
| PAN No. 1 | 64 | 2.2 | 4.4 |
| PAN No. 2 | 76 | 2.6 | 3.7 |
| PAN No. 3 | 64 | 1.5 | 6.4 |
| PAN No. 4 | 58 | 2.1 | 4.6 |

$\sigma_0$ = 9.6 mS cm$^{-1}$ at 30 °C.

charge–discharge process. The MacMullin number ($N_M$), which is defined as the ratio of the conductivity of the pure electrolyte to that of separator containing electrolyte, could be used in order to evaluate the influence of the separator on the high rate capability [1,8], i.e. lower $N_M$ value of separator would be preferred for the high power application. The porosities, ionic conductivities and the $N_M$ value of the separators are summarized in Table 2. The $N_M$ value was calculated by following equation [9]:

$$N_M = \frac{\sigma_0}{\sigma_{eff}} \quad (1)$$

where $\sigma_0$ and $\sigma_{eff}$ are the conductivities of electrolyte and separator containing electrolyte, respectively. The PAN nonwovens made of the 250 nm fibers showed slightly higher $N_M$ value than the PAN nonwovens made of the 380 nm fibers. The higher $N_M$ values of the PAN Nos. 3 and 4 could be ascribed to their high gurley values, low porosities and smaller pore size. The $N_M$ values of the PAN No. 1–4 were 4.4, 3.7, 6.4 and 4.6, respectively. It is clear that the PAN nonwovens possessed less than half of the $N_M$ value of the Celgard membrane because of higher porosities and lower gurley values.

Fig. 3(a) shows a comparison of the initial charge–discharge curves at the 0.5*C* rate for the test cells using the Celgard membrane and the PAN nonwovens. The cells showed stable charge–discharge curves with discharge capacities of about 120–125 mAh g$^{-1}$ based on the weight of $LiCoO_2$. In our preliminary charge–discharge test, a cell using a polyolefin nonwoven (35 μm in thickness) made of polyolefin fibers with about 2 μm in diameter showed unstable voltage profile above 4.0 V at charge process probably due to the micro-short circuit by formation of lithium dendrite. It is noticeable that any unstable voltage profile was not observed for the cells with the PAN nonwovens with almost the same or less thickness to the previous polyolefin nonwoven. The stable voltage profiles would be ascribed to the small pore size of the PAN nonwovens. Fig. 3(b) shows cycle stabilities of the test cells. The cells using the PAN nonwovens showed better cycling performances than that of the Celgard one. The obtained discharge capacities and capacity retention ratios of the cells after 250 cycles are summarized in Table 3.

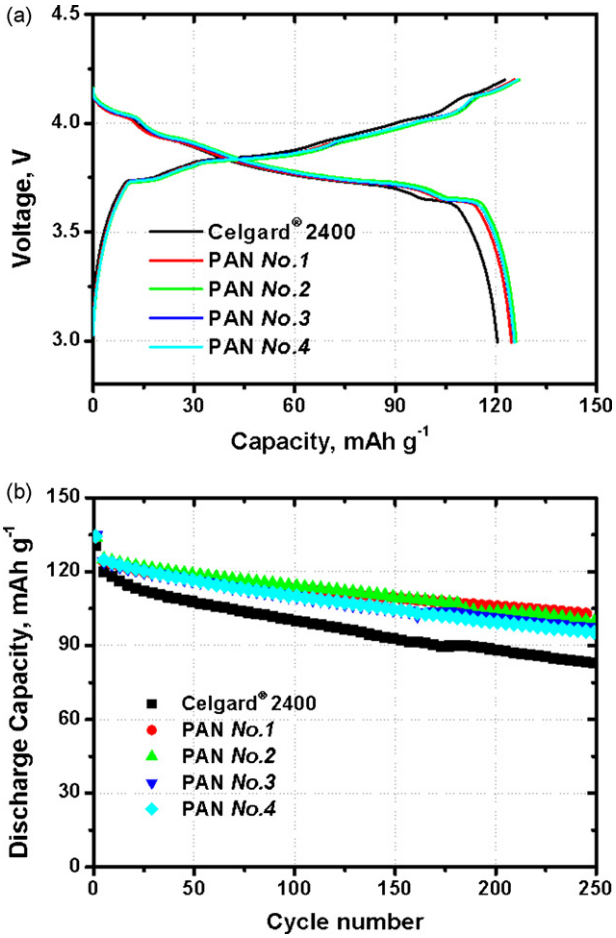


**Fig. 3.** (a) Initial charge–discharge curves for the cells with the Celgard membrane and the PAN nonwoven membranes. (b) Discharge capacities *vs.* cycle numbers of the test cells at the 0.5*C* rate.

**Table 3**
Summarized data of charge–discharge performances and charge transfer resistances estimated by EIS measurements for the cells

| Separators | Capacity | | | Resistance, Ω | | |
|---|---|---|---|---|---|---|
| | Initial (mAh g$^{-1}$) | At 250 cycle (mAh g$^{-1}$) | Capacity retention ratio after 250 cycles (%) | $R_{CT\,(initial)}$ | $R_{CT\,(250)}$ | $\Delta R_{CT}$ |
| Celgard® 2400 | 120.4 | 82.7 | 68.7 | 8.0 | 20.0 | 12.0 |
| PAN No. 1 | 124.5 | 102.7 | 82.5 | 7.2 | 14.2 | 7.0 |
| PAN No. 2 | 125.9 | 99.8 | 79.3 | 7.2 | 12.5 | 5.3 |
| PAN No. 3 | 125.3 | 97.1 | 77.5 | 5.5 | 14.2 | 8.7 |
| PAN No. 4 | 125.4 | 95.4 | 76.1 | 6.7 | 12.1 | 5.3 |

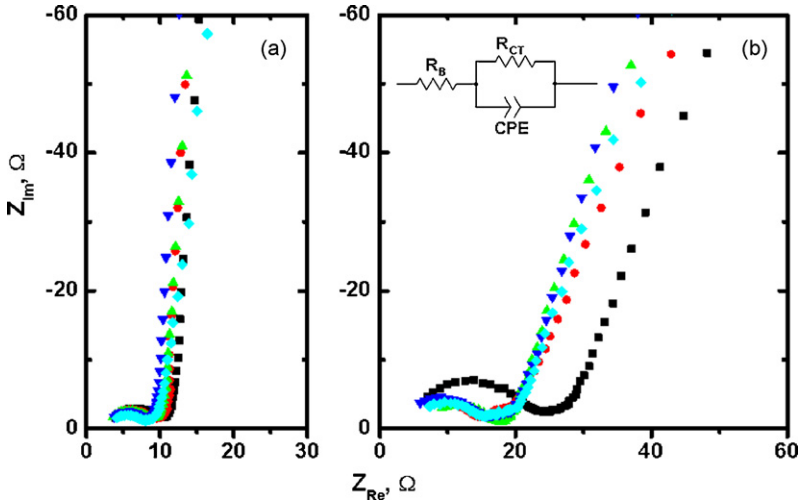


**Fig. 4.** Nyquist plots for the cells with the Celgard membrane (■), PAN No. 1 (●), PAN No. 2 (▲), PAN No. 3 (▼) and PAN No. 4 (◆) measured at (a) the fresh state and (b) at the end of the cycle test.

In order to investigate the variation of cell impedances during cycle test, the electrochemical impedance spectroscopy measurement was carried out for the cells at the fresh state and the end of the charge–discharge test. Fig. 4(a) and (b) shows Nyquist plots of the cells measured at the fresh state and the end of the cycle test, respectively. The spectra consist of a semicircle in the high-middle frequency region and a straight line in the low frequency region. The semicircle corresponds to the charge-transfer process, accompanied with migration of the lithium ion at the electrode/electrolyte interface. The straight line in the low frequency region corresponds to the diffusion process of lithium ion in the electrode. The charge-transfer resistances for the spectra were estimated by fitting the semicircle in the spectra based on an equivalent circuit (the inset of Fig. 4(b)). The components in the equivalent circuit, such as $R_B$, $R_{CT}$ and CPE represent a bulk resistance including the resistance of the electrolyte and electrode, a charge-transfer one and a capacitative constant-phase element, respectively. The estimated charge-transfer resistances of the cells are summarized in Table 3. The charge-transfer resistances of the cells at the fresh state were almost the same. However, a clear difference on them was observed after the end of cycle test. The charge-transfer resistances of the PAN nonwovens were in the range of 12–14 Ω, whereas that of the Celgard membrane showed 20 Ω. The different increasing ratio ($\Delta R_{CT}$) of the charge-transfer resistance between the PAN nonwovens and the Celgard membrane would be ascribed to the difference in the retainability of the liquid electrolyte in the separator. The higher porosities and better wettabilities of the PAN nonwovens than that of the Celgard one would help to retain large amount of electrolyte in the separator, facilitating the migration of lithium ion at the electrode/electrolyte boundary and then suppressing the increase in charge-transfer resistance during cycle test. The better cycleability for the cells with PAN nonwovens than that with the Celgard membrane would be understood in terms of lower increasing ratio of the charge-transfer resistances.

Fig. 5 shows SEM photograph of the PAN No. 1 after 250th cycle. As compared with the fresh PAN nonwoven (see Fig. 1(a)), the morphology of the PAN nonwoven almost unchanged after the cycling test as shown in Fig. 5.

Fig. 6 shows rate capabilities of the cells with the separators. The cell with the Celgard membrane showed capacity retention ratio of about 90% at the 1*C* rate, and then decreased rapidly with increasing the *C* rate up to 8*C* rate. The obtained ratio at the 2, 4, 8*C* rate were 81, 42 and 7%, respectively. The cells with the PAN nonwovens showed

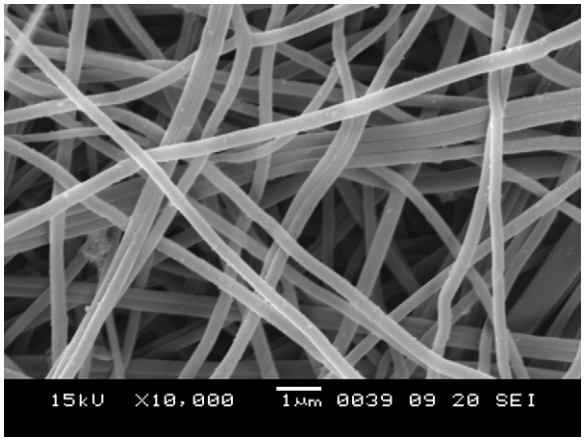


**Fig. 5.** SEM photograph of the PAN No. 1 after the charge–discharge test.

outstanding rate capabilities. Up to the 4*C* rate, the cells retained more than 90% of the capacities obtained at the 0.2*C* rate. The ratios were higher more than 2 times that for the Celgard one at the same *C* rate. A clear difference on the capacity retention ratio of the cells with the PAN nonwovens was observed at the 8*C* rate. The ratios

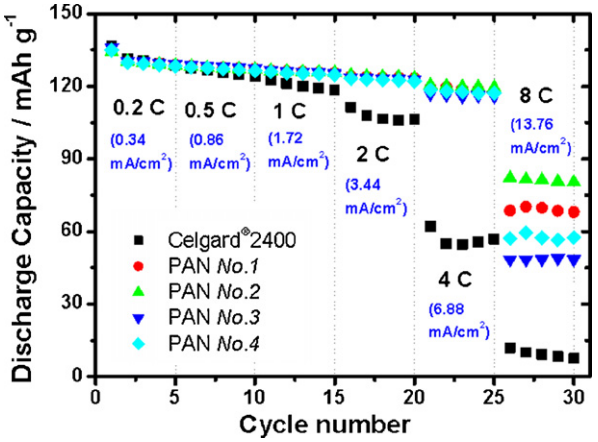


**Fig. 6.** Results of rate capability tests for the cells with the Celgard membrane and the PAN nonwovens.

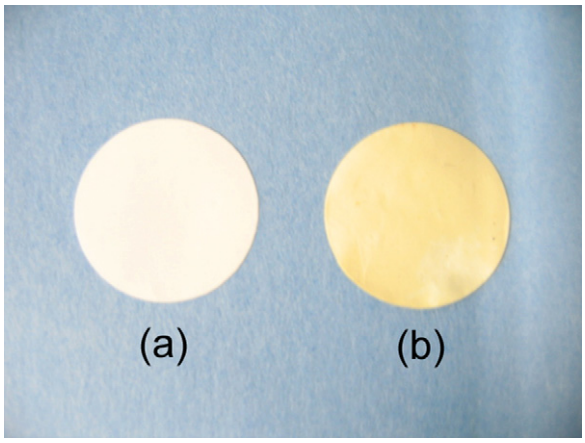


**Fig. 7.** Photographs of the PAN nonwovens (a) before and (b) after hot oven test at 200 °C for 60 min.

of the PAN No. 1–4 at the 8*C* rate were 53%, 62%, 37% and 45%, respectively. There is a tendency that the separator with lower $N_M$ value exhibits higher rate capability.

### 3.3. Thermal properties

In our previous paper [5], we have reported that the PAN nonwoven is thermally stable in the temperature range of room temperature to 250 °C on the differential scanning calorimetry (DSC) measurement. Fig. 7(a) and (b) shows shape of the PAN nonwovens before and after the hot oven test at 200 °C for 1 h, respectively. The PAN nonwoven did not show any shrinkage at 200 °C, even though the color of the PAN nonwoven changed from white to light brown. Subsequently, hot oven tests using the CR-2032 coin type cell after charging up to 4.2 V were carried out for the PAN nonwoven, compared with the cell with the Celgard membrane. After the hot oven test at 120 °C for 1 h, the shape of the separators was almost unchanged and vigorous voltage changes were not observed during the test. Next, the hot oven test was carried out at 150 °C. The variations of voltage profiles *versus* time for the cells during the hot oven test are presented in Fig. 8. Unfortunately, both of the cells showed sudden voltage drop after 10 (Celgard membrane) and 14 min (PAN nonwoven), respectively, from start of the test, probably corresponding to the short circuit. The short circuits could be caused by the shrinkage of the separators at high temperature of 150 °C in the electrolyte.

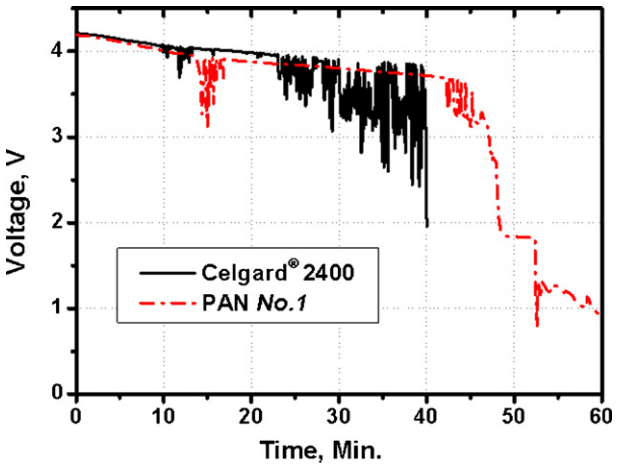


**Fig. 8.** The voltage profiles for the cells with Celgard membrane and PAN No. 1 during the hot oven test at 150 °C.

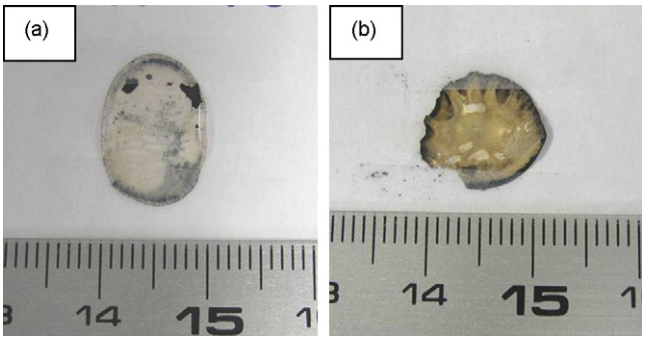


**Fig. 9.** Photographs of the (a) Celgard membrane and the (b) PAN nonwoven after the hot oven test at 150 °C.

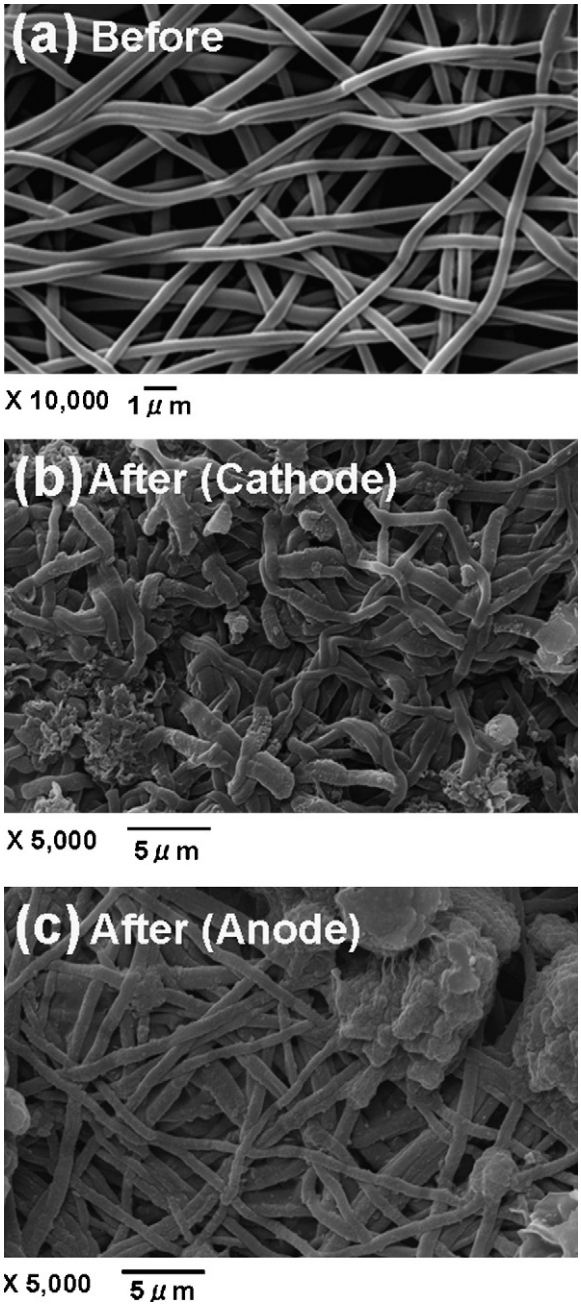


**Fig. 10.** SEM photographs of the PAN nonwoven membrane before and after the hot oven test. (a) Before, (b) after (cathode) and (c) after (anode).

After the tests, we have observed macro- and micro(only for the PAN No. 1)-morphological changes for the separators as presented in Figs. 9 and 10, respectively. Shrinkages were observed for both of the separators. The Celgard membrane showed uniaxial shrinkage of about 30% along the machine direction (Fig. 9(a)). The PAN nonwoven also showed isotropic shrinkage of about 26% and some warping (Fig. 9(b)). Fig. 10(a–c) shows micro-morphologies of the PAN No. 1 before and after the hot oven test at 150 °C. The SEM photographs revealed that the fine PAN fibers became thicker by swelling and bonded each other, giving rise to thermal shrinkage of the separator, and also collapse the porous structure in the nonwoven. Interestingly, a clear difference between cathode side and anode one was observed for the morphologies of the PAN fibers. The fibers which contacted with the cathode (Fig. 10(b)) became crook, whereas the fibers which contacted with the anode (Fig. 10(c)) kept their morphologies, though the observed diameters of the fibers for both the sides of PAN nonwoven were almost the same. The difference in morphological changes between the cathode side and the anode one would bring about the warping of the PAN nonwoven due to their different shrinkage ratio. The reason for the crook of the fibers could be attributed to oxidation of the fibers under the oxidative condition on the charged cathode at high temperature of 150 °C. This result indicates that the thermal stability of the PAN nonwoven membrane at the high temperature of 150 °C is not sufficient yet.

## 4. Conclusions

The microporous polyacrylonitrile nonwoven have been manufactured by electrospinning technique. The PAN nonwovens exhibited similar pore size to the conventional microporous membrane with homogeneous pore size distribution. The PAN nonwovens with small mean pore sizes were successfully manufactured by using nano-fibers of 250 and 380 nm in diameter without remarkable decrease in its porosity. The PAN nonwovens showed higher ionic conductivities than that of the Celgard membrane because of their high porosities. The cells with the PAN nonwovens showed better cycle lives at the 0.5*C* rate with smaller increase in the charge-transfer resistances than that with the Celgard membrane during charge–discharge test. Moreover, the cells with the PAN nonwovens exhibited better rate capabilities than that with the Celgard membrane. The PAN nonwovens are thermally stable at 120 °C, but become unstable at 150 °C. Now, we are improving the thermal stability of the nonwoven by combination of thermally stable nonwoven webs as a frame.

## References

[1] P. Azora, Z. Zhang, Chem. Rev. 104 (2004) 4419.
[2] J. Saunier, F. Alloin, J.Y. Sanchez, G. Caillon, J. Power Sources 119–121 (2003) 451.
[3] Y.M. Lee, J.W. Kim, N.S. Choi, J.A. Lee, W.H. Seol, J.K. Park, J. Power Sources 139 (2005) 235.
[4] F.G.B. Ooms, E.M. Kelder, J. Schoonman, N. Gerrits, J. Smedinga, G. Callis, J. Power Sources 97–98 (2001) 598.
[5] T.H. Cho, T. Sakai, S. Tanase, K. Kimura, Y. Kondo, T. Tarao, M. Tanaka, Electrochem. Solid-State Lett. 10 (7) (2007) A159.
[6] C. Zhang, X. Yuan, L. Wu, Y. Han, J. Sheng, Eur. Polym. J. 41 (2005) 423.
[7] S.S. Zhang, J. Power Sources 164 (2007) 351.
[8] K.M. Abraham, Electrochim. Acta 38 (1993) 1233.
[9] K.K. Patel, J.M. Paulsen, J. Desilvestro, J. Power Sources 122 (2003) 144.